Fusion Engineering and Design 85 (2010) 1711–1715

Contents lists available at ScienceDirect

Fusion Engineering and Design

journal homepage: www.elsevier.com/locate/fusengdes

Integrated simulation of tritium permeation in solid breeder blankets

Hongjie Zhang*, Alice Ying, Mohamed A. Abdou

Fusion Science and Technology Center, University of California, Los Angeles, 420 Westwood Plaza, Los Angeles, CA 90095-1597, USA

ARTICLE INFO

Article history:
Available online 3 June 2010

Keywords:
Tritium permeation
Purge convection
Breeding blanket
3D Model

ABSTRACT

Numerical simulation of co-permeation of tritium and hydrogen from breeding zones to the coolant in the helium cooled pebble-bed blanket is performed in this paper. 3D multi-species convection–diffusion models integrated with thermal-fluid analysis in porous media are assessed and then used to estimate the associated tritium permeation for a solid breeder blanket module. Benchmark calculations give a reasonable agreement on the co-permeation rates with the experimental data. Simulation in a TBM unit show that purge gas flow can strongly affect tritium transport, increasing the purge flow velocity is an effective method to reduce tritium permeation to the coolant. In the case where hydrogen is added to the purge gas stream to promote tritium release, the co-permeation of H_2, T_2, and HT are taken into account in the permeation simulation, results show that permeation flux of T–T molecules is reduced due to the effect of co-permeation of hydrogen.

1. Introduction

Tritium permeation to the coolant should be limited in order to minimize economic and safety penalties associated with tritium processing systems. Therefore, it is very important to estimate tritium permeation under relevant operating conditions for fusion energy. Key variables that can strongly affect the tritium permeation from the breeder zone to the coolant, such as the tritium release rate, temperature, and solid breeder microstructure have been identified [1]. In addition, characteristics of the purge gas, such as its composition and flow rate, also play an important role on tritium permeation. In the current phase of research and development, there is a strong incentive to develop predictive capabilities in order to understand the experimental data, and to provide a necessary tool for fusion blanket design analysis. In this concern, the primary purpose of this paper is to develop new models which attempt to give an accurate description of the multi-physics phenomena that characterize tritium permeation in complex geometries and under realistic reactor-like conditions; and to develop a computer code to predict the tritium permeation as a function of different variables and for a wide range of operating conditions. Calculation of tritium permeation has recently been presented as a 2D convection–diffusion model to account for the effects of purge stream convection [2]. The proposed model in this paper coupled several physical phenomena, such as multi-species convection–diffusion in purge gas and coolant, diffusion through the structure, and thermal-fluid analysis in porous media. A 3D Sc/Tetra-based CFD code has been developed based on this model. Additionally, the distribution of tritium generation rate and nuclear heating rate are also taken into account in the model. Calculation results are in reasonable agreement with Kizu's [3] experimental results for both single species permeation and multi-species permeation. Implantations for a Test Blanket Module (TBM) in the fusion environment under different conditions were also performed to provide a predictive capability of tritium and hydrogen permeation in the helium cooled pebble-bed blanket.

2. Physical model

The model presented here includes the following controlling physical processes: (1) convection–diffusion of T_2, H_2, and HT in the purge gas with packed bed flow. (2) Tritium movement across metal surfaces by molecular dissociation to solid solution and the reverse process of molecular recombination to the gas phase of the metal. (3) Diffusion of dissolved atomic tritium and hydrogen through the structure. (4) Convection–diffusion of T_2, H_2, and HT in the coolant.

The model geometry is defined in three regions as shown in Fig. 1: the pebble-bed breeding region (1) with helium purge gas flowing through it, the TBM structure (2) and the helium coolant region (3). In the model, the purge gas region has a length of $l = 0.368$ m, a pebble-bed width of $w_1 = 11$ mm near the First Wall and 18 mm at the other end and height of $h = 0.128$ m, a structure thickness of $w_2 = 1.25$ mm, and a coolant channel width of $w_3 = 3$ mm and height of $h_3 = 5$ mm.

H_2, T_2, and HT are transported by diffusion and convection in the two fluid regions, whereas diffusion is the only transport mechanism in the structure phase. The system can be described by the

* Corresponding author. Tel.: +1 310 825 8824.
E-mail address: zhjbook@gmail.com (H. Zhang).

0920-3796/$ – see front matter © 2010 Elsevier B.V. All rights reserved.
doi:10.1016/j.fusengdes.2010.05.018

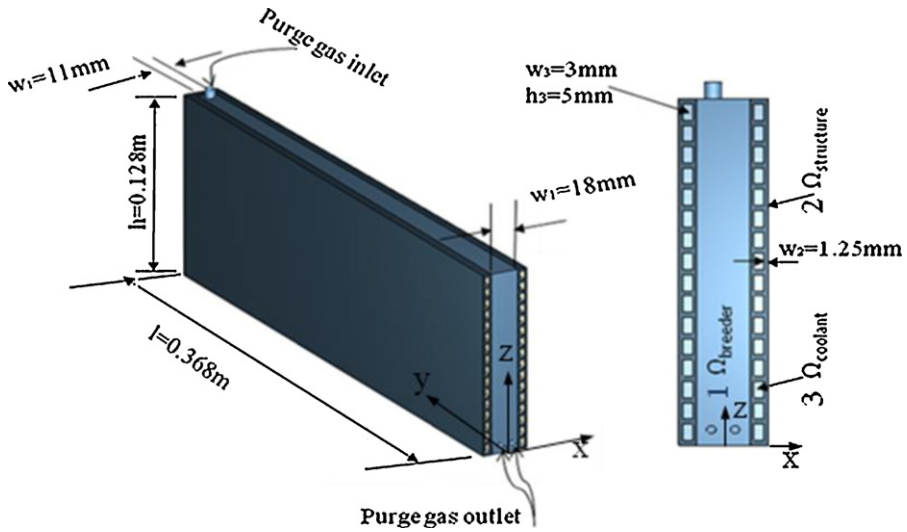

Fig. 1. Diagram of the blanket module.

following mass transport equations:

$$\frac{\partial c_1}{\partial t} + \boldsymbol{u}\nabla c_1 = D_1\nabla^2 c_1 + Q_c \tag{1}$$

$$\frac{\partial c_2}{\partial t} = D_2\nabla^2 c_2 \tag{2}$$

$$\frac{\partial c_3}{\partial t} + \boldsymbol{U}\nabla c_3 = D_3\nabla^2 c_3 \tag{3}$$

In these equations, c_i and i denote the molar concentration of the species (mol/m^3) and the diffusion coefficient (m^2/s) in the respective phases. The velocities (m/s) in the respective flow regions are denoted by **u** and **U**. Time is represented by t and Q_c is the tritium generation rate in the breeder blanket.

To obtain the convective part of the tritium flux in the breeding zone, velocity distributions are introduced by solving the N–S equation based on Brinkman model of flow in a packed bed. Considering the wall effects, which reflects the variations of porosity and tritium transport in the bed near the wall regions, the calculation uses the following governing equations [4]:

$$\frac{\partial \rho \boldsymbol{u}}{\partial t} + \boldsymbol{u}\nabla\rho\boldsymbol{u} = \frac{\mu}{\varphi*}\nabla^2\boldsymbol{u} - \nabla p - \frac{\mu \boldsymbol{u}}{K*} \tag{4}$$

$$\varphi* = \varphi^*_\infty \left\{1 + C_1 \exp\left[-\frac{N_1(d)}{d_p}\right]\right\} \tag{5}$$

$$K* = K^*_\infty \left\{1 + C_2 \exp\left[-\frac{N_2(d)}{d_p}\right]\right\} \tag{6}$$

$$\varphi^*_\infty = 0.4, \quad K^*_\infty = 1.185\times 10^{-3} d_p^2, \quad C_1 = 1, \quad N_1 = 2,$$
$$C_2 = 20, \quad N_2 = 4 \tag{7}$$

In these equations, φ^* and K^* represent porosity and flow permeability, φ^*_∞ and K^*_∞ are the porosity and flow permeability in the bulk of the packed bed, the particle diameter is equal to d_p = 1 mm, and d is the distance from the wall.

The processes that govern the permeation of solute gas atoms in structures are highly temperature dependent. Therefore, the thermal response needs to be determined by solving energy conservation equations:

$$\frac{\partial \rho_1 C_{p1} T_1}{\partial t} + \boldsymbol{u}\nabla\rho_1 C_{p1} T_1 = \lambda_1\nabla^2 T_1 + \dot{q} \tag{8}$$

$$\rho_2 C_{p2}\frac{\partial T_2}{\partial t} = \lambda_2\nabla^2 T_2 \tag{9}$$

$$\rho_3 C_{p3}\frac{\partial T_3}{\partial t} + \rho_3 C_{p3}\boldsymbol{U}\nabla T_3 = \lambda_3\nabla^2 T_3 \tag{10}$$

where ρ, C_p, and λ are the density, heat capacity and conductivity respectively and $\dot{q}$ is the local volumetric heating rate.

An important key feature of the proposed model is the characterization of the surface region between gas and structure. For the gas–structure interface, tritium movement across the metal surface is often governed by molecular dissociation to solid solution and the reverse process of molecular recombination to the gas phase of the metal. In many situations, tritium movement through the surface approaches equilibrium and the surface concentrations are determined by the appropriate solubility relationships, such as Sieverts' law. For metals, Sieverts' law relates the equilibrium concentration of solute atoms in the metal to the tritium partial pressure above the surface of the metal. The relation is

$$c_2 = S{P_1}^{1/2} \quad \text{at purge–structure interface} \tag{11}$$

$$c_2 = S{P_3}^{1/2} \quad \text{at structure–coolant interface} \tag{12}$$

where, c_2 is the concentration of mobile atomic species s at the surface, P_1 and P_3 are the partial pressures, and $S = 0.364\exp(-0.277\,\text{eV}/kT)$ mol/m^3 Pa$^{0.5}$ is the solubility coefficient for Sieverts' law. Additionally, accurate boundary conditions at the gas–structure interface are necessary to ensure the flux continuity conditions.

$$-D_1\frac{\partial c_1}{\partial n} = -D_2\frac{\partial c_2}{\partial n} \quad \text{at purge–structure interface} \tag{13}$$

$$-D_2\frac{\partial c_2}{\partial n} = -D_3\frac{\partial c_3}{\partial n} \quad \text{at structure–coolant interface} \tag{14}$$

where n is the normal direction of the interface.

Because there are discontinuities in the concentration profile at the boundaries between liquid and solid phases, appropriate boundary conditions using the stiff-spring method [5] have been applied to define continuous flux conditions, at the same time, ensure the discontinuities of the concentrations.

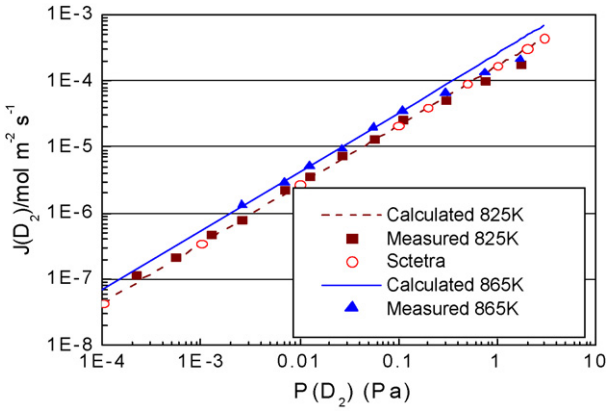

Fig. 2. D_2 permeation flux as a function of the upstream deuterium pressure.

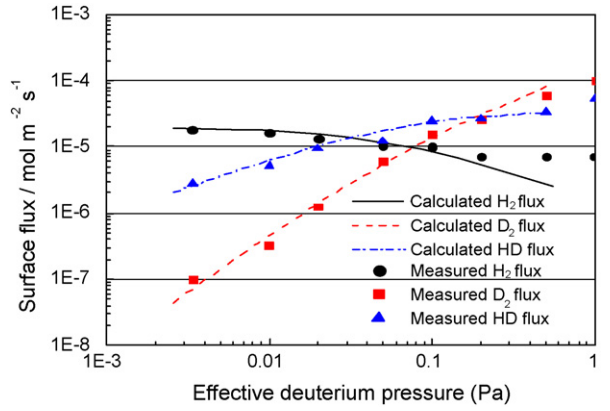

Fig. 3. HD, H_2, D_2 permeation flux in co-permeation measurements as a function of the effective deuterium pressure ($P_D = P_{D_2} + P_{HD}/2$) and at a fixed value of effective H_2 pressure ($P_H = P_{H_2} + P_{HD}/2 = 0.063$ Pa).

3. Numerical results and discussion

3.1. Validation

Kizu's [2] experiments have been chosen for the validation analysis. In the experiment, permeations of deuterium through a palladium membrane, which was accompanied by co-permeation of hydrogen, were performed. Two cases have been selected for the calibration; we first replicate the calibration experiments of permeation of D_2 only through the Pd membrane (thickness of 0.025 mm, temperatures of 825 K and 865 K). The calculated permeation flux shown in Fig. 2 are almost as good as the experimental results, although the calculated permeation flux gets a little worse as the deuterium pressure gets higher. For the co-permeation of *H* and *D* through Pd membrane (0.025 mm, 825 K), the calculated and experimental permeation flux are plotted and compared in Fig. 3. These results are consistent with the observations of experiment that permeation appears to be nearly first-order in the effective deuterium pressure *P* at low pressure but tends to become proportional to $P^{1/2}$ as driving pressure increases.

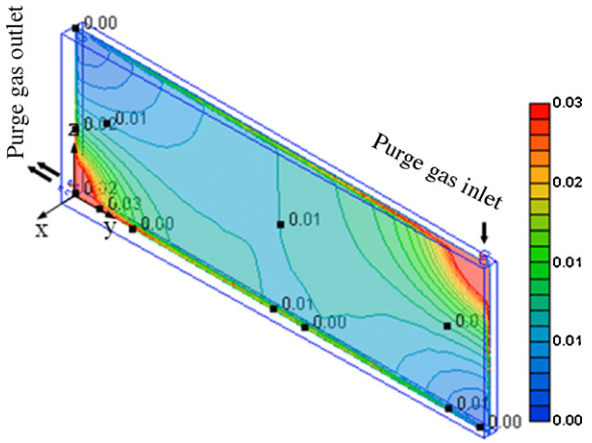

Fig. 5. The velocity field in the purge gas region at the $x = 0.012$ m plane.

3.2. Simulation of TBM unit

Two cases, tritium only permeation and co-permeation of tritium and hydrogen, were performed for the 3D TBM unit (Fig. 1). The distribution of nuclear heating rate and tritium production rate in the radial direction are shown in Fig. 4. The key variables, such as velocity profile, tritium concentration, tritium permeation flux, and other parameters of interest, were analyzed in this paper.

3.2.1. Single permeation

Using the multi-physics model proposed in this paper, computations were first performed for tritium only permeation in a TBM unit. Fig. 5 shows the velocity field in the purge gas region at the $x = 0.012$m plane. Velocity near the inlet and outlets area is much higher than the average velocity of 0.01 m/s in the center of the purge gas area, and low velocity fields appears in the other two corners. Fig. 6 shows the velocity along *x*-direction at $y = 0.2$ m and $z = 0.0672$ m. It can be seen that the velocity near the wall reaches 3 times the center velocity due to wall effects.

Fig. 7 illustrates the tritium concentration profile in the purge gas region at the $x = 0.012$ m plane, and Fig. 8 shows the compar-

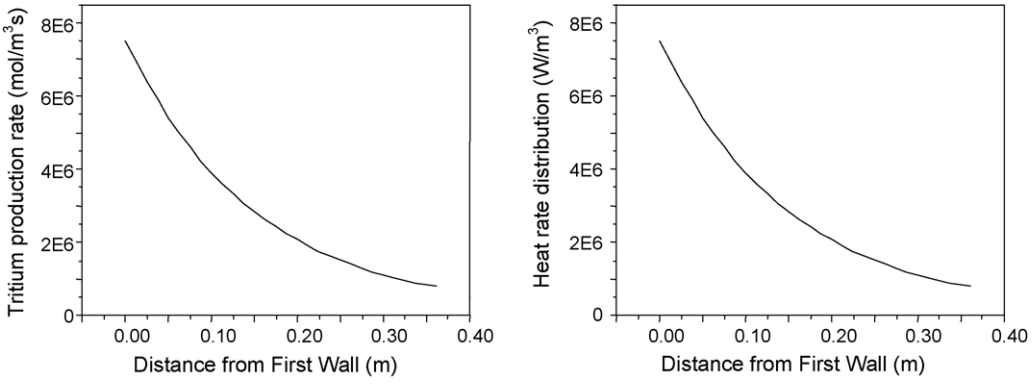

Fig. 4. Nuclear heating rate and tritium production rate as a function of distance in the radial direction.

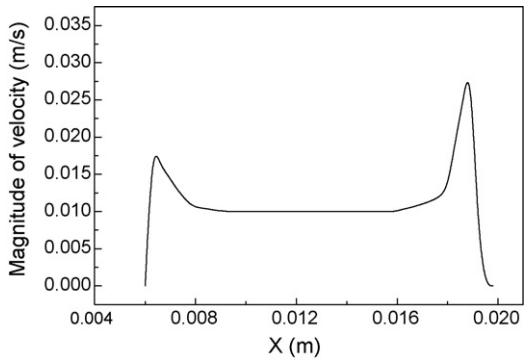

Fig. 6. The velocity along x-direction at $y = 0.2$ m and $z = 0.0672$ m.

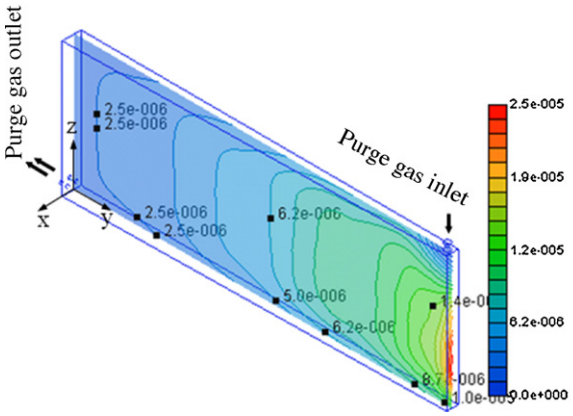

Fig. 7. Tritium concentration in the purge gas region at the $x = 0.012$ m plane.

ison of tritium concentration with wall effects and without wall effects along x-direction at $y = 0.2$ m and $z = 0.0672$ m. Comparing the velocity profile and tritium concentration profile, it can be seen that the "M-shape" velocity profile near the wall region in a porous flow has a slight benefit in preventing tritium permeation due to higher convection effect near the wall, but under the given conditions, this additional advantage is relatively small.

Fig. 9 shows the tritium permeation flux at the purge gas–structure interface. The tritium flux is higher near the first wall and lower near the outlets, since the tritium production rate and temperature are relatively higher near the first wall. The total permeation in the calculated region is 3.62e−12 mol/s, nearly 6.4% of the total production.

To evaluate the effect of flow rate on tritium permeation, three different inlet purge gas mass flow rates (1.0e−6 kg/s, 1.5e−6 kg/s,

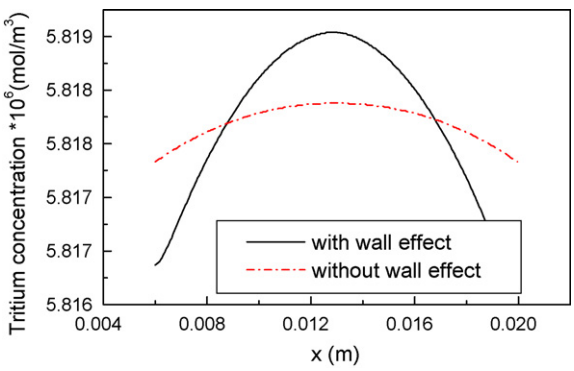

Fig. 8. The tritium concentration with and without wall effects along the x-direction at $y = 0.2$ m and $z = 0.0672$ m.

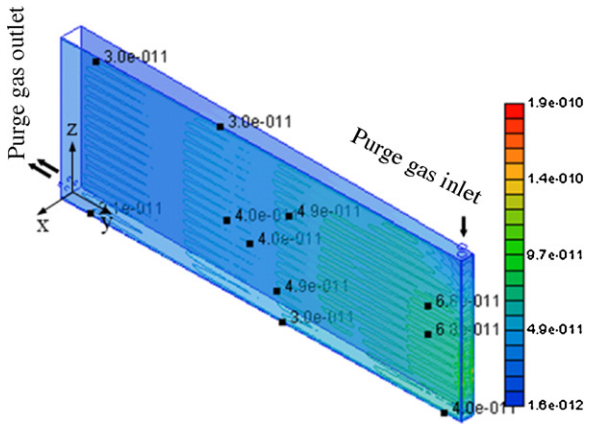

Fig. 9. The tritium permeation flux at the purge gas–structure interface.

and 1.8e−6 kg/s) were chosen for comparison. The corresponding average velocity along the $y = 0.2$ m plane are 0.007 m/s, 0.01 m/s, and 0.012 m/s. Fig. 10 shows the total tritium permeation flux through the purge gas–structure interface at different flow conditions. The data shows that purge gas flow rate plays an important role in reducing tritium permeation. However, the penalty is an increase in purge gas hydraulic pressure drop and subsequent pumping power. Certainly, there is a window for optimizing the purge gas flow conditions to reduce tritium permeation while minimizing the pressure drop.

3.2.2. *Tritium permeation in conditions of hydrogen co-permeation*

If certain amounts of H_2 are introduced into the purge gas region from the purge gas inlet, three molecular species H_2, T_2, and HT will be produced in the purge gas region. All of them are allowed to permeate through structure. Then, assuming local chemical equilibrium for the system under consideration, the final concentrations of H_2, T_2, and HT in the gas phase are governed by the following relationship:

$$\frac{C_{HT}^2}{C_{T_2} \times C_{H_2}} = K_{eq} \tag{15}$$

Fig. 11 shows the permeation flux of H_2, T_2, and HT molecules as functions of the amount of H_2 added from the purge gas inlet. It is clear that the permeation rate of these respective species strongly depends on the amount of H_2 present. The rate of H–H and H–T recombination both increased, while that of T–T recombination decreases. If 100 wppm of H_2 exists in the inlet purge gas, the total

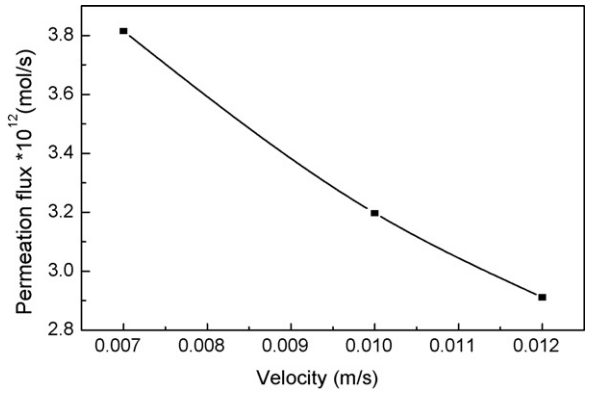

Fig. 10. The total tritium permeation flux through the purge gas–structure interface at different average flow velocities.

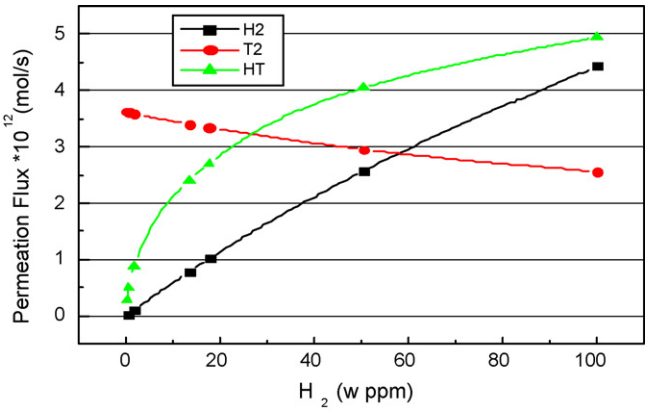

Fig. 11. Permeation flux of H_2, T_2, and HT molecules as a function of the amount of H_2 added.

permeation T_2 molecules is 2.56e−12 mol/s, a drop of nearly 29% compared to the T_2 only case.

4. Conclusion

A 3D multi-species convection–diffusion model integrated with thermal-fluid analysis in porous media were assessed for correlation with experimental data. Benchmark calculations agree well with experimental results for both single permeation and co-permeation cases. Tritium permeation from the breeding zone to the coolant in the TBM unit is simulated for both T_2 only and H_2, T_2 co-permeation models. The results show that the "M-shape" velocity profile near the wall region in a porous flow has a slight benefit in preventing tritium permeation due to the higher convection effects near the wall. The influence of convection on permeation was evaluated under different mass flow rates and the results showed that higher mass flow rate decreased tritium permeation. Permeation of tritium in conditions of hydrogen co-permeation was also evaluated with different concentrations of H_2. Results show that the permeation flux of T–T molecules will drop due to the effect of hydrogen co-permeation.

References

[1] Blanket Comparison and Selection Study (Final Report), Argonne National Laboratory, ANL/FPP-84-1 (1984).
[2] W. Guo, A. Ying, M. Ni, M. Abdou, Influence of 2D and 3D convection–diffusion flow on tritium permeation in helium cooled solid breeder blanket units, Fusion Engineering & Design 81 (8-14) (2006) 1465–1470.
[3] K. Kizu, A. Pisarev, T. Tanabe, Co-permeation of deuterium and hydrogen through Pd, J. Nucl. Mater. 289 (2001) 291–302.
[4] P. Cheng, C.T. Hsu, Fully-developed, forced convective flow through an annular packed-sphere bed with wall effects, Int. J. Heat Mass Transfer 29 (1986) 1843–1853.
[5] Multicomponent Transport: Separation through Dialysis, COMSOL Inc., 2007.